Reconciling experimental and numerical data: techniques of nonlinear seakeeping code validation

Leigh McCue*, William Belknap**, and Bradley Campbell**

Abstract

In this paper the authors apply qualitative and quantitative approaches in an effort to validate numerical nonlinear seakeeping codes. The work begins with a presentation of safe basin boundaries and integrity curves focusing primarily upon variations in wave steepness and roll/roll velocity state space variables for a realistic ship operating in stern quartering seas. The simulated results are compared to experimental data acquired in the Maneuvering and Seakeeping Basin (MASK) at the Naval Surface Warfare Center, Carderock Division. The study then discusses the use of analytical methods, such as Lyapunov exponents, to quantitatively validate a numerical simulation to experimental results.

1 Introduction

Due to the crucial sensitivity to initial conditions of capsize as well as the binary nature of vessel instability, *ie* capsize or non-capsize, 'validating' a large amplitude numerical simulation tool is a nontrivial endeavor. Approaches to compare numerical and experimental results of nonlinear ship motions include qualitative means, such as comparison of safe basins and integrity curves (Soliman & Thompson, 1991; Thompson, 1997; Spyrou & Thompson, 2000), multi-dimensional integrity curves (McCue & Troesch, 2003) or quantitative methods such as comparison of Lyapunov exponents (Murashige *et al.*, 2000; McCue & Troesch, 2004), correlation dimension (Murashige & Aihara, 1998b) and system entropy (Bulian, 2005).

Safe basins and integrity curves have been used by the naval architecture community to define the separatrix between capsize and non-capsize regions and illustrate the crucial sensitivity of capsize to initial conditions. As defined in works by Thompson and collaborators, safe basins portray roll/roll velocity state space marking capsize as black regions and non-capsize as white regions. An integrity curve represents a series of safe basins by plotting the ratios of safe area to total area over a sweep of some critical parameter, such as wave height (Soliman & Thompson, 1991; Thompson, 1997; Spyrou & Thompson, 2000). This approach has been extended to multiple degrees of freedom with multi-dimensional integrity curves and probabilistic methods have been incorporated to define realistic initial condition values (McCue & Troesch, 2003; McCue & Troesch, 2005).

The use of Lyapunov exponents to study capsize has been discussed in the literature for both naval architecture and nonlinear dynamics. In recent years the Lyapunov exponent has been calculated from equations of motion for the mooring problem (Papoulias, 1987), single degree of freedom capsize models (Falzarano, 1990; Arnold *et al.*, 2003), single degree of freedom flooded ship models (Murashige & Aihara, 1998a; Murashige & Aihara, 1998b; Murashige *et al.*, 2000) and works studying the effects of rudder angle while surf-riding as it leads to capsize (Spyrou, 1996). Because the Lyapunov exponent, which measures the rate of exponential convergence or divergence of nearby trajectories, provides a quantitative value, it can be used as a tool to directly compare the accuracy of a numerical model to experimental runs (McCue & Troesch, 2004). Rather than attempting to qualitatively evaluate a numerical simulation through assessing its predictive capability of the binary event capsize/non-capsize, the Lyapunov exponent can be used to demonstrate that a numerical model is likely simulating the same form of chaos as experiments.

This paper presents a discussion of both qualitative and quantitative approaches to validating numerical simulations through consideration of experiments and FREDYN simulation of a pre-contract DDG-51 hullform (model 5514). Results from scale experiments conducted in the Maneuvering and Seakeeping (MASK) Basin at the Naval Surface Warfare Center, Carderock Division are presented and com-

*Aerospace and Ocean Engineering, Virginia Tech, mccue@vt.edu

**Seakeeping Division, Naval Surface Warfare Center, Carderock Division, william.belknap@navy.mil, bradley.campbell@navy.mil

pared to full-size simulated time series.

2 Qualitative: Safe Basins & Integrity Curves

The numerical simulation tool, FREDYN, was used to generate safe basins for a pre-contract design of DDG-51 represented by model 5514 shown in Figure 1. All simulations were conducted in stern quartering seas (waves 45^o off the stern), at a Froude number of 0.40, for wave length to ship length ratios of $0.75 \leq \lambda/L \leq 1.50$ and wave steepness ranging from $0 \leq h/\lambda \leq \frac{1}{7}$. The simulated ship was free to move in six degrees of freedom and employed an autopilot control attempting to replicate the autopilot used for the MASK model basin experiments. The scale ratio of full length (as simulated) to model length was $L_S/L_M = 46.6$

For each λ/L and h/λ of interest, numerical simulations were conducted over a range of roll and roll velocities from $-88^o \leq \phi \leq 88^o$ and $-50^o/s \leq \dot{\phi} \leq 50^o/s$ respectively at a resolution of 1^o and $1^o/s$ increments. Each run was simulated for 1000 seconds (full scale), which corresponds to approximately 22-36 cycles, or until the point of capsize. Black and white regions indicate capsize and non-capsize respectively. Sample safe basins are given in Figure 2.

Integrity curves are generated by plotting the ratio of safe area to total area over a range of wave heights. These values are normalized to 1 at a wave height of zero. Figures 3-6 present integrity curves for model 5514 at ratios of $\lambda/L = 0.75$, 1.0, 1.25, and 1.5 with $Fn = 0.40$ in stern quartering seas. The experimental conditions which lead to capsize or non-capsize are noted on each plot with a vertical line.

The plots clearly follow the behavior initially noted by Thompson and collaborators for a single degree of freedom model, namely the vessel encounters a critical wave height at which it experiences a rapid loss of stability, *i.e.*'cliff's of Dover' (Soliman & Thompson, 1991; Thompson, 1997; Spyrou & Thompson, 2000). A few additional points are worth highlighting. Note that the integrity curves consistently rise above the normalized integrity value of 1.0 at small wave heights. This result is consistent with the findings of McCue and Troesch (2003) for a simplified three-degree of freedom model. It is foreseeable that under certain circumstances some amount of wave forcing provides a corrective, stabilizing force upon the system. Additionally, Figure 5 seems to indicate that FREDYN overpredicts capsize due to the existence of a non-capsize experimental case occurring well into the region of zero integrity. However, when considering time to capsize, it becomes clear that due to the necessary exposure time to result in capsize, many experimental runs will not capsize because of the finite nature of even the largest maneuvering testing facility. The issue of limited experiment run length is further exacerbated by any initial heading error, due to the time required to return to desired heading. For example, Figure 7 presents frames from video taken for the anomalous non-capsizing case shown in Figure 5. As shown in the video frames, the experimental model was regularly in a near-capsize state with emerged bilge keels and propellers and often became captured by the wave motion into headings deviating from stern-quartering seas towards beam seas. It is probable that the model would have capsized if the experiment continued over a longer duration. One must also recognize that the location of the steep region in the integrity curve will shift with variations in other degree of freedom initial conditions (McCue & Troesch, 2003).

As a theoretical aside, the observed behavior that capsize can occur over a relatively wide range of times for similar runs, may be an indicator of transient chaos rather than a deterministic behavior (Eckhardt & Faisst, 2005). For a numerical model, Soliman and Thompson demonstrate that capsize typically occurs within 16 cycles of steady-state excitation (1991). While the results in this work are consistent with that conclusion, nearly identical runs do not necessarily capsize at nearly identical times. That is, neighboring initial conditions often capsize after substantially different times. Figure 8 presents a plot of time to capsize for $h/\lambda = 0.0732$. As can be seen, capsizes occur in the first few steps of the numerical simulation as well as at times in excess of 900 seconds of full scale simulated data.

3 Quantitative: Lyapunov Exponents

Quantitative comparisons between experiments and FREDYN output were made via Lyapunov exponent spectrum comparisons. To begin, the d-dimensional phase portraits of both experimental and numerical attractors were reconstructed from delay coordinates as: $\mathbf{x(t)} = \{\phi(t), \phi(t+\tau), \phi(t+2\tau), ..., \phi(t+(d-1)\tau)\}$ where τ is the delay time (Parlitz, 1992). The delay time for all experimental and simulated cases was chosen to be approximately 1/4 the response

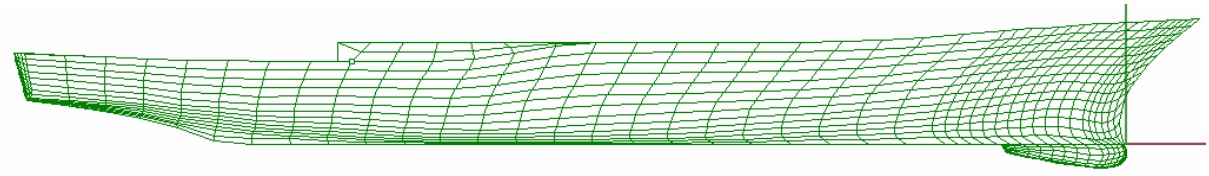

Figure 1: Model 5514 mesh.

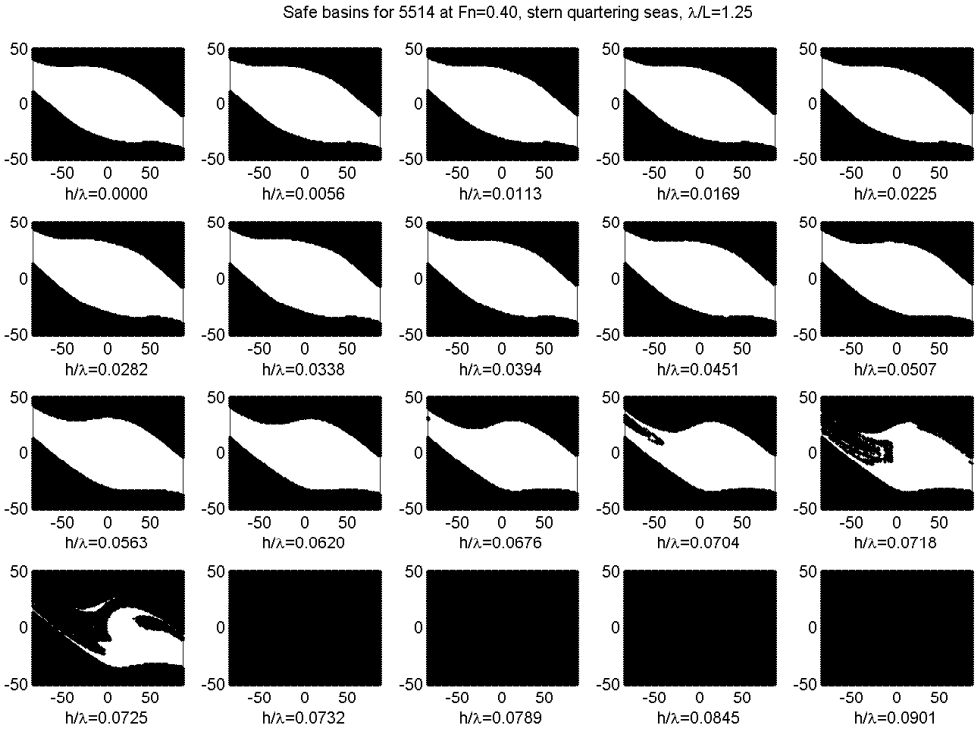

Figure 2: Safe basins for pre-contract hull 5514 at Fn=0.40, $\lambda/L = 1.25$ in stern quartering seas.

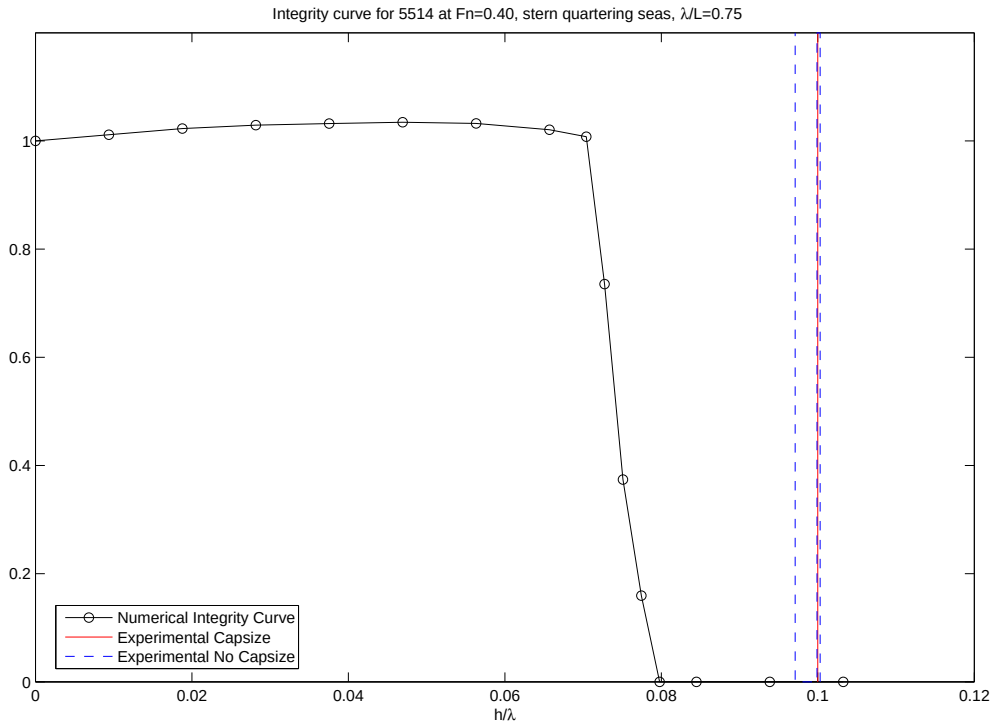

Figure 3: Integrity curve for model 5514 at Fn=0.40, $\lambda/L = 0.75$ in stern quartering seas.

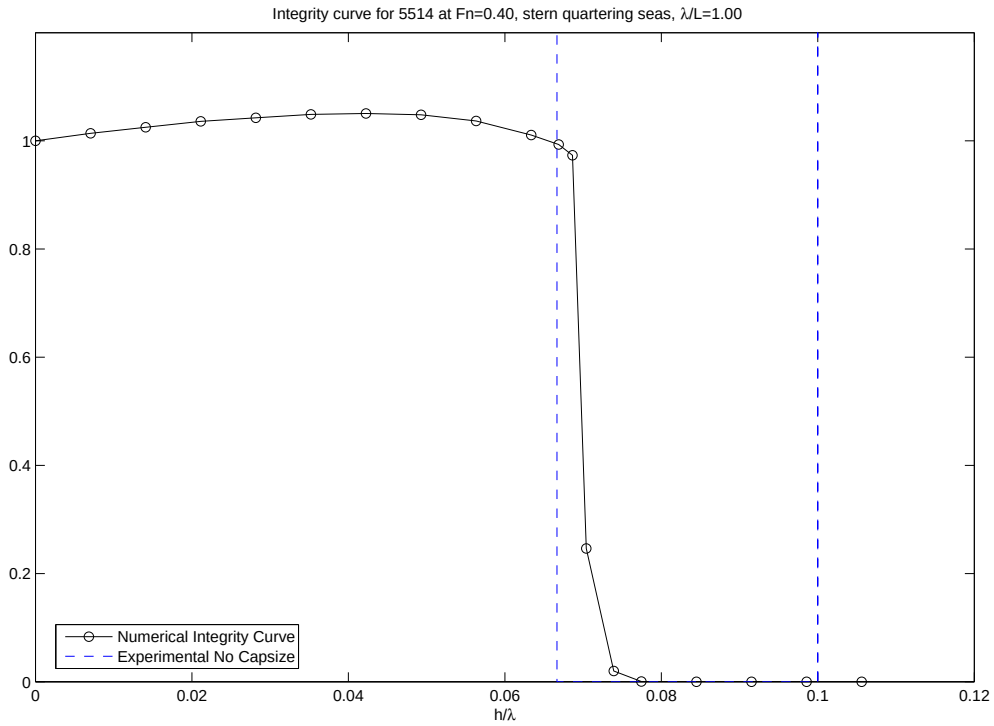

Figure 4: Integrity curve for model 5514 at Fn=0.40, $\lambda/L = 1.00$ in stern quartering seas.

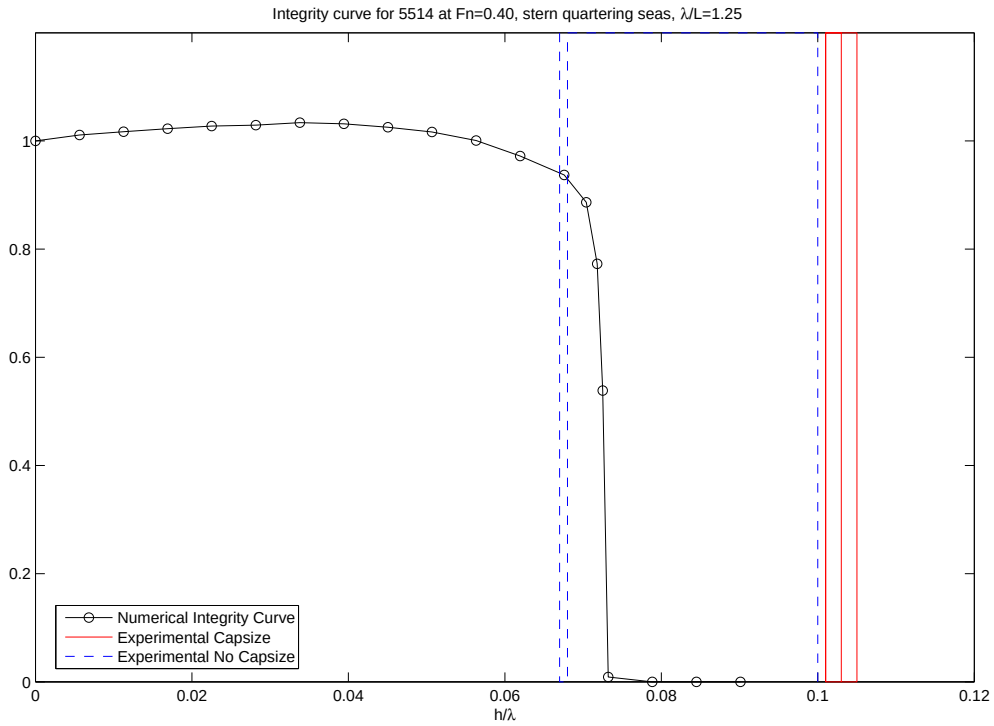

Figure 5: Integrity curve for model 5514 at Fn=0.40, $\lambda/L = 1.25$ in stern quartering seas.

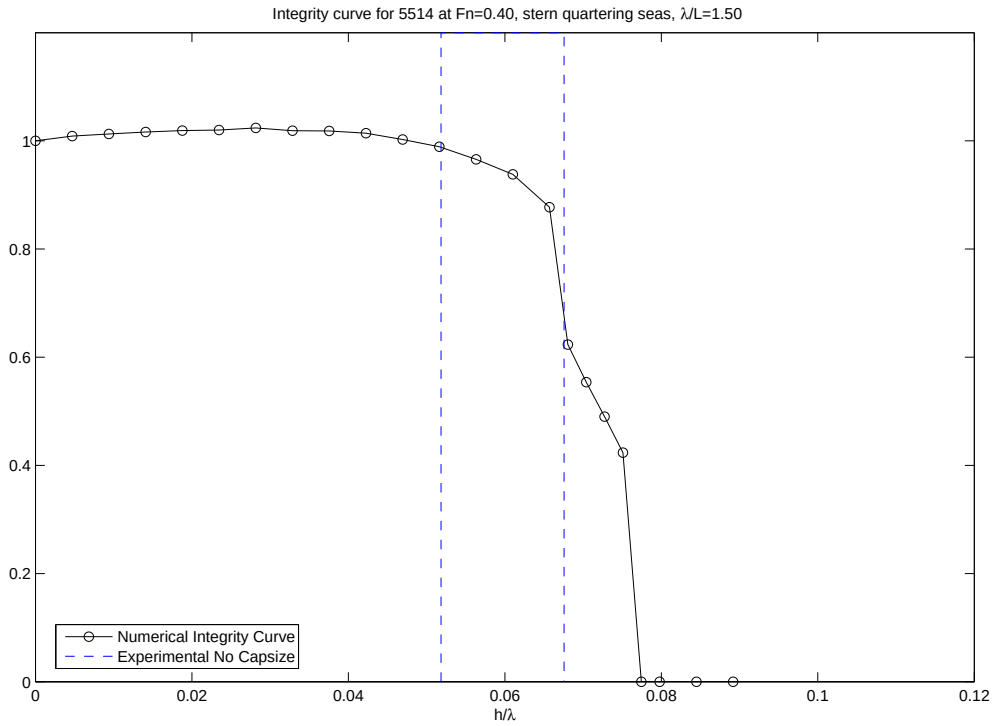

Figure 6: Integrity curve for model 5514 at Fn=0.40, $\lambda/L = 1.50$ in stern quartering seas.

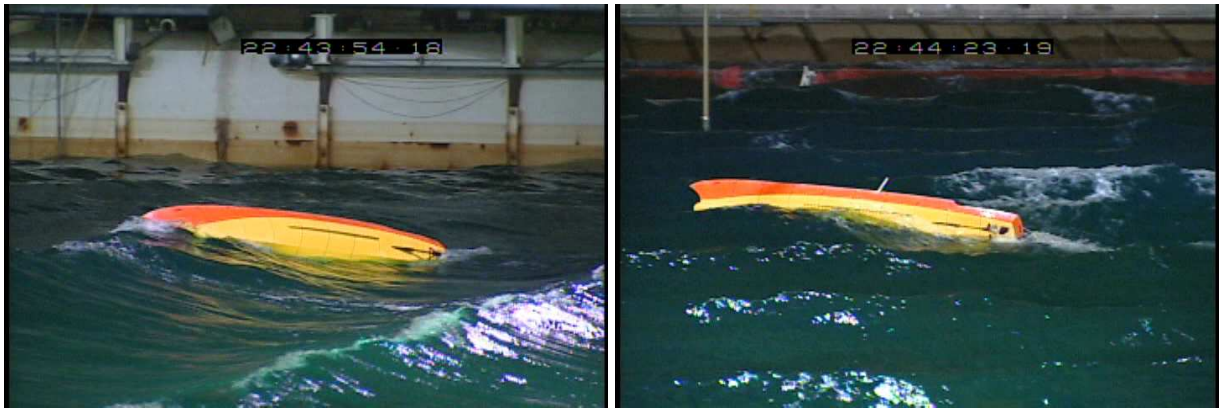

Figure 7: Video frames near beginning and end of model 5514, experimental run 329 at Fn=0.40, $\lambda/L = 1.252$, $h/\lambda = 1/9.972$ released in stern quartering seas.

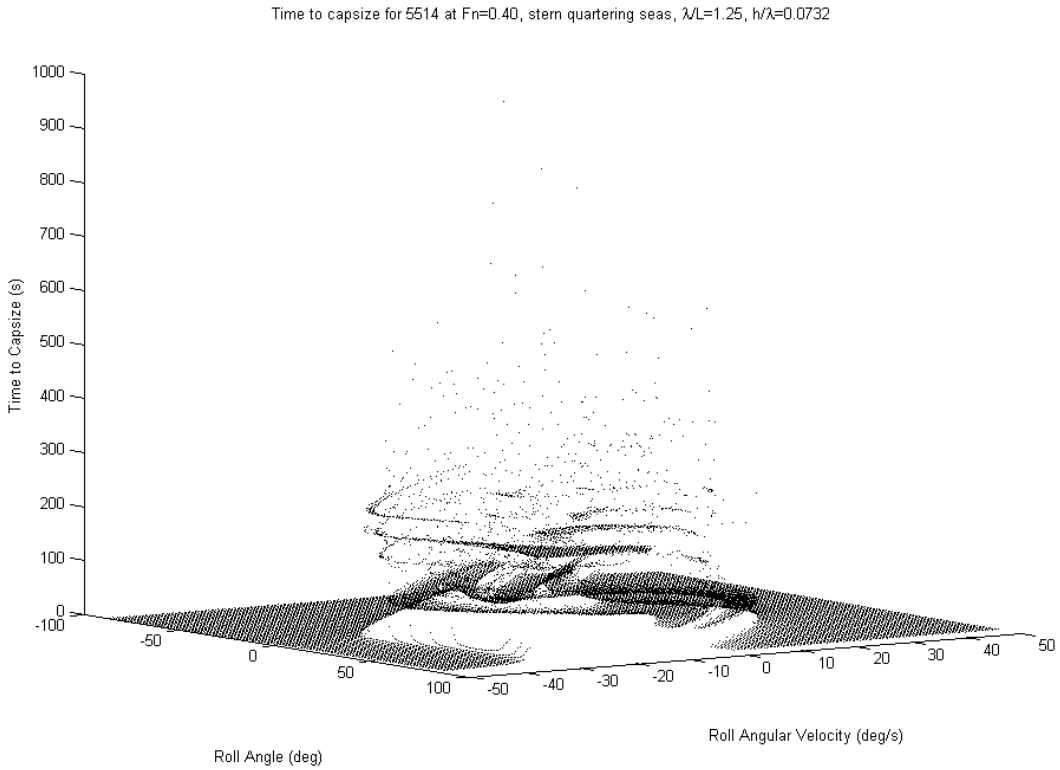

Figure 8: FREDYN simulated, full-scale, time to capsize for model 5514 at Fn=0.40, $\lambda/L = 1.25$, $h/\lambda = 0.0732$ in stern quartering seas.

period of the model and simulation considered separately, rather than choosing a single delay time for both; $\tau_{exp} = 3.98$s (full-scale) and $\tau_{sim} = 9$s. While the model typically responded at periods near its natural period, the simulated full scale ship often responded near the encounter period. In such a case, the model would most likely have acquired a different heading leading to resonant roll conditions. The autopilot is not as effective in this situation, due to instrumentation and physical limitations, and the model would be less likely to reacquire the desired heading during the limited run time. Therefore, to accurately capture the attractor dynamics, the delay was chosen based upon the observed response of the system and within a parameter range where estimated Lyapunov exponents were robust to change in delay time rather than strictly scaling delay time with the square root of the scale ratio.

Phase portraits of the reconstructed attractor from both the experimental and numerical cases are presented in Figure 9. As is apparent, the three-dimensional reconstructed phase-space exhibits different behavior between experiments and numerical simulation. While it is possible this is a result of the embedding process, this variation may indicate a difference in the fundamental physics captured by the numerical and experimental data. Details as to the characterization of vessel responses through examination of embedding reconstructed state-space can be found in Murashige and Aihara (1998b).

A method based upon the algorithm developed by Sano and Sawada (1985) was implemented in Matlab to calculate Lyapunov exponent spectra from the model 5514 experimental and numerical time series. For verification, maximal Lyapunov exponents were checked using the Kantz (1994) algorithm contained in the TISEAN package (2000). Details of these methods can be found in the noted papers or in texts such as Kantz and Schreiber (2004).

When calculating Lyapunov exponents from a single variate time series, one must choose an embedding dimension, d, that is the dimension of the reconstructed phase space encompassing the dynamics of the system. While the Sano and Sawada algorithm is relatively robust with respect to both embedding dimension and delay, it is important to isolate a realistic range of embedding dimension values and identify any spurious exponents which may arise. By plotting Lyapunov exponent versus embedding dimension it is feasible to determine an optimal embedding dimension range over which Lyapunov exponent values are consistent. Additionally, Parlitz suggests calculating the Lyapunov spectrum for the reversed time series to identify spurious exponents (1992). He argues that true exponents reverse sign upon time reversal.

In Figure 10 Lyapunov spectra for experimental and numerical cases are shown plotted versus embedding dimension. One expects to observe a number of exponents, and time reversed exponents, converge to finite values indicating true Lyapunov exponents. Those outliers which remain outliers over a range of embedding dimensions are likely spurious exponents arising from the embedding process. The simulated data demonstrate exceedingly small positive, zero, and negative exponents and it is not clear that the full spectrum has been defined at an embedding dimension of 8.

The experimentally obtained data, scaled by $\sqrt{(L_M/L_S)}$ result in positive, zero, and negative exponents, without clear convergence of the spectrum at an embedding dimension of 7. It is probable that this is due to the high dimensional nature of ship motions. The attractor dynamics are not fully captured in 7-dimensional phase-space; for a six degree of freedom system, even operating on the assumption that heave and pitch responses trace their static equilibria (Umeda & Hamamoto, 2000), it is likely that substantially larger embedding dimensions, on the order of 10-12, are necessary for accurate results. The length of the time series precludes substantially increasing embedding dimension for this analysis. As embedding dimension increases, the difficulty in finding sufficient neighboring trajectories with which to calculate Lyapunov exponents without sacrificing precision, also increases.

While the range of Lyapunov exponent values for experimental and numerical time series are within the same broad region, it is observed that the maximal Lyapunov exponent for experimental runs is significantly larger than those of numerical cases. The numerical cases demonstrate little, if any, chaotic behavior with only very small positive Lyapunov exponents. The largest Lyapunov exponents for 8 experimental cases and 14 numerical simulations are given in Table 1 as measured with an embedding dimension of 5. While the precise Lyapunov exponent behavior one wishes to see for validation purposes, namely near exact matching of Lyapunov spectra, is not available, a higher dimensional analysis would be necessary to conclusively state that the simulations likely capture, or fail to capture, the relevant physics of the experimental system.

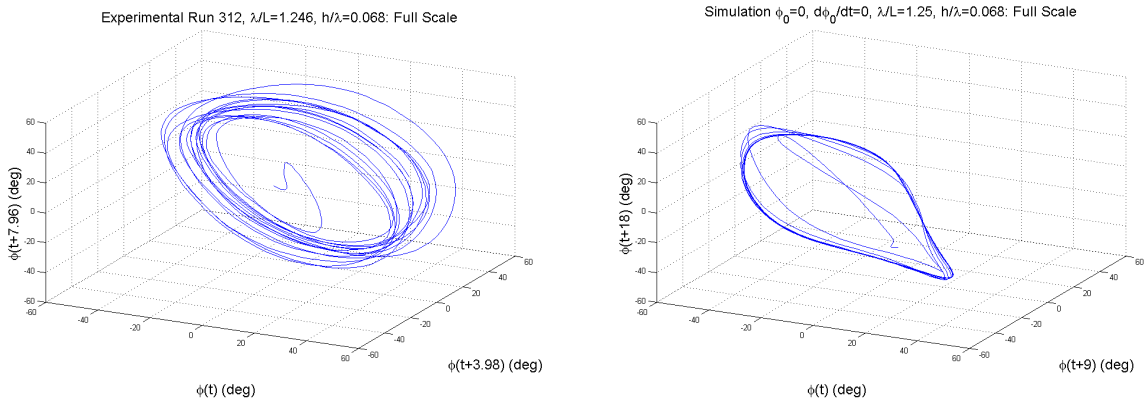

Figure 9: Reconstructed attractor phase portrait from sample experimental (left) and numerical (right) data for model 5514.

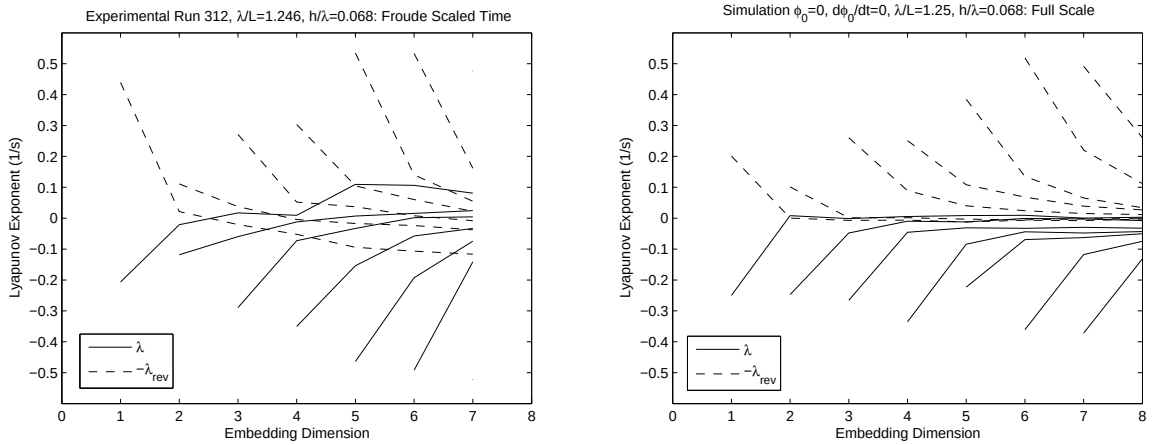

Figure 10: Lyapunov spectrum as a function of embedding dimension from sample experimental (left) and numerical (right) data for model 5514. The spectra for the original roll time series is plotted via solid lines and the spectra for the reversed time series is plotted with dashed lines.

Experimental Data				**Simulated Data**				
Run #	h/λ	λ/L	*Lyap. Exp. (1/s)*	ϕ *(deg)*	$\dot{\phi}$ *(deg/s)*	h/λ	λ/L	*Lyap. Exp. (1/s)*
400	0.0518	1.498	0.0303	-20	-20	0.068	1.25	0.0115
239	0.0667	1.000	0.0296	-20	0	0.068	1.25	0.0085
313	0.0671	1.248	0.0186	-20	20	0.068	1.25	0.0001
312	0.0681	1.246	0.1093	0	-20	0.068	1.25	0.0115
418	0.0971	0.773	0.1571	0	0	0.068	1.25	0.0085
417	0.0999	0.750	0.1084	0	20	0.068	1.25	0.0070
281	0.1000	1.000	0.0929	20	-20	0.068	1.25	0.0147
329	0.1003	1.252	0.0880	20	0	0.068	1.25	0.0075
				20	20	0.068	1.25	0.0086
				-20	-20	0.073	1.25	0.0152
				0	-20	0.073	1.25	0.0134
				0	0	0.073	1.25	0.0125
				20	-20	0.073	1.25	0.0148
				20	0	0.073	1.25	0.0113

Table 1: Table of largest Lyapunov exponents for experimental and numerical cases, $d = 5$.

4 Conclusions

This paper details qualitative and quantitative approaches for validating numerical simulations in comparison to experimentation. It is not the aim of this work to validate FREDYN specifically, but rather to discuss validation tools for numerical simulations. The results presented herein are exploratory and as such cannot conclusively validate or invalidate FREDYN as a simulation tool based upon comparison to model 5514 experimental data. However, a few conclusions can be drawn along with suggestions for future work.

- Identification of steep regions in integrity curves can provide explanation for seemingly inconsistent experimental behavior. Due to computation-time constraints only variations in roll/roll velocity initial conditions were considered with initial conditions for the surge, sway, heave, pitch, and yaw degrees of freedom equal to zero. Variations in these initial conditions can shift the location of the steep region of the integrity curve (McCue & Troesch, 2003) and all initial conditions are not equally likely to occur (McCue & Troesch, 2005), therefore other quantitative, system-dependent, validation tools were also investigated.

- Time to capsize becomes an important variable to consider in comparison of experimental and numerical results. Experimental runs expected to capsize may not as a result of finite experimental basin size limitations.

- Through examination of the embedding reconstruction of the attractor state-space it appears that different behavior is captured in the numerical and experimental cases. Delay embedding state space portraits can be used to catalogue different forms of ship response (Murashige & Aihara, 1998b) and pose another qualitative means of comparing experimental and numerical results.

- Comparison of Lyapunov exponents for numerical and experimental time series offer a validation tool. Using delay reconstruction, only a single variate time series is required, however long time series are required for high dimensional systems in order to accurately compute full Lyapunov spectra and compare experimental to numerical values. For the comparison presented in this paper, both experimental and numerical cases resulted in small positive Lyapunov exponents, though there was no overlap between exponents calculated from simulated time series and those of experimental data.

5 Acknowledgements

The authors wish to acknowledge the support of the Hydromechanics Department of the Carderock Division of the Naval Surface Warfare Center and the ONR-ASEE Summer Faculty Research Program.

References

Arnold, L., Chueshov, I., & Ochs, G. 2003. *Stability and capsizing of ships in random sea-a survey.* Tech. rept. 464. Universität Bremen Institut für Dynamicsche Systeme.

Bulian, Gabriele. 2005. Nonlinear parametric rolling in regular waves-a general procedure for the analytical approximation of the GZ curve and its use in time domain simulations. *Ocean Engineering*, **32**, 309–330.

Eckhardt, Bruno, & Faisst, Holger. 2005. *Dynamical systems and the transition to turbulence.* preprint received via private communication.

Falzarano, Jeffrey M. 1990. *Predicting complicated dynamics leading to vessel capsizing.* Ph.D. thesis, University of Michigan.

Hegger, Rainer, Kantz, Holger, Schreiber, Thomas, & *et al.* 2000. *TISEAN 2.1, Nonlinear Time Series Analysis.* `http://www.mpipks-dresden.mpg.de/~tisean/TISEAN_2.1/index.html`.

Kantz, Holger. 1994. A robust method to estimate the maximal Lyapunov exponent of a time series. *Physics Letters A*, **185**, 77–87.

Kantz, Holger, & Schreiber, Thomas. 2004. *Nonlinear time series analysis.* Second edn. Cambridge University Press.

McCue, Leigh S., & Troesch, Armin W. 2003 (September). The effect of coupled heave/heave velocity or sway/sway velocity initial conditions on capsize modelling. *In: 8th International Conference on the Stability of Ships and Ocean Vehicles.*

McCue, Leigh S., & Troesch, Armin W. 2004 (November). Use of Lyapunov exponents to predict chaotic vessel motions. *In: 7th International Ship Stability Workshop.*

McCue, Leigh S., & Troesch, Armin W. 2005. Probabilistic determination of critical wave height for a multi-degree of freedom capsize model. *Ocean Engineering*, **32**, 1608–1622.

Murashige, S., Yamada, T., & Aihara, K. 2000. Nonlinear analyses of roll motion of a flooded ship in waves. *Philosophical Transactions of the Royal Society of London A*, **358**, 1793–1812.

Murashige, Sunao, & Aihara, Kazuyuki. 1998a. Coexistence of periodic roll motion and chaotic one in a forced flooded ship. *International Journal of Bifurcation and Chaos*, **8**(3), 619–626.

Murashige, Sunao, & Aihara, Kazuyuki. 1998b. Experimental study on chaotic motion of a flooded ship in waves. *Proceedings of the Royal Society of London A*, **454**, 2537–2553.

Ott, Edward, Sauer, Tim, & Yorke, James (eds). 1994. *Coping with Chaos.* New York: John Wiley and Sons.

Papoulias, Fotis Andrea. 1987. *Dynamic analysis of mooring systems.* Ph.D. thesis, Department of Naval Architecture and Marine Engineering, University of Michigan, Ann Arbor, MI.

Parlitz, Ulrich. 1992. Identification of true and spurious Lyapunov exponents from time series. *International Journal of Bifurcation and Chaos*, **2**, 155–165. Reprinted in (Ott *et al.*, 1994).

Sano, M, & Sawada, Y. 1985. Measurement of Lyapunov spectrum from a chaotic time series. *Physical Review Letters*, **55**(10).

Soliman, Mohamed S., & Thompson, J.M.T. 1991. Transient and steady state analysis of capsize phenomena. *Applied Ocean Research*, **13**(2).

Spyrou, K.J. 1996. Homoclinic connections and period doublings of a ship advancing in quartering waves. *Chaos*, **6**(2).

Spyrou, K.J., & Thompson, J.M.T. 2000. The nonlinear dynamics of ship motions: a field overview and some recent developments. *Philosophical Transactions of the Royal Society of London: Mathematical, Physical, and Engineering Sciences*, **358**(1771), 1735–1760.

Thompson, J.M.T. 1997. Designing against capsize in beam seas: Recent advances and new insights. *Appl Mech Rev*, **50**(5).

Umeda, N., & Hamamoto, M. 2000. Capsize of ship models in following/quartering waves: physical experiments and nonlinear dynamics. *Philosophical Transactions of the Royal Society of London: Mathematical, Physical, and Engineering Sciences*, **358**(1771), 1883–1904.